

UCLA

UCLA Previously Published Works

Title

Therapeutic Response Assessment of High-Grade Gliomas During Early-Phase Drug Development in the Era of Molecular and Immunotherapies

Permalink

<https://escholarship.org/uc/item/34z2h6rk>

Journal

The Cancer Journal, 27(5)

ISSN

1528-9117

Authors

Ellingson, Benjamin M
Wen, Patrick Y
Cloughesy, Timothy F

Publication Date

2021-09-01

DOI

10.1097/ppo.0000000000000543

Peer reviewed



Published in final edited form as:

Cancer J. 2021 ; 27(5): 395–403. doi:10.1097/PPO.0000000000000543.

Therapeutic response assessment of high-grade gliomas during early phase drug development in the era of molecular and immunotherapies

Benjamin M. Ellingson¹, Patrick Y. Wen², Timothy F. Cloughesy³

¹UCLA Brain Tumor Imaging Laboratory (BTIL), Center for Computer Vision and Imaging Biomarkers, Department of Radiological Sciences, David Geffen School of Medicine, University of California Los Angeles, Los Angeles, CA

²Center for Neuro-Oncology, Dana-Farber Cancer Institute, Harvard University, Boston, MA

³UCLA Neuro Oncology Program, Department of Neurology, David Geffen School of Medicine, University of California Los Angeles, Los Angeles, CA

Abstract

Several new therapeutic strategies have emerged over the past decades to address unmet clinical needs in high grade gliomas, including targeted molecular agents and various forms of immunotherapy. Each of these strategies requires addressing fundamental questions depending on the stage of drug development, including ensuring drug penetration into the brain, engagement of the drug with the desired target, biologic effects downstream from the target including metabolic and/or physiologic changes, and identifying evidence of clinical activity that could be expanded upon to increase the likelihood of a meaningful survival benefit. The current review article highlights these strategies and outlines how imaging technology can be used for therapeutic response evaluation in both targeted and immunotherapies in early phases of drug development in high grade gliomas.

Current Therapeutic Landscape for High Grade Gliomas: Molecular and Immunotherapies

Several new therapeutic strategies have emerged over the past 20 years to address unmet clinical needs, particularly in recurrent disease in which there is no consensus as to the standard of care as no therapeutic options that have produced substantial survival benefit¹, including the development of specific targeted agents and various forms of immunotherapy. Each of these therapeutic strategies and stages of clinical trial evaluation have their own unique questions, potential complications, and specific mechanisms of action that can be distinctively addressed using imaging techniques and approaches. For example, early phase trials using targeted agents might benefit from having information about blood-brain barrier

*Corresponding author Benjamin M. Ellingson, Ph.D., Director, UCLA Brain Tumor Imaging Laboratory (BTIL), Professor of Radiology and Psychiatry, Departments of Radiological Sciences and Psychiatry, David Geffen School of Medicine, University of California, Los Angeles, 924 Westwood Blvd., Suite 615, Los Angeles, CA 90024 (bellingson@mednet.ucla.edu), Phone: 310-481-7572, Fax: 310-794-2796.

permeability, drug penetration into the brain, or downstream physiological changes known to accompany the treatment, whereas later stage trials might be more focused on tumor shrinkage, growth rate changes using serial measures of bulk enhancing or non-enhancing tumor, and overall survival (Fig. 1). During immunotherapy development investigators may have unique challenges, including differentiation of treatment-related inflammation (i.e. “pseudoprogression”) from progressive disease and spatial differentiation and/or quantification of particular immune cells (e.g. CD8+ or macrophages with a particular polarity) from active tumor cells within a heterogeneous enhancing mass. The current review article will highlight some of these strategies and outline how imaging technology can be used for therapeutic response evaluation in both targeted and immunotherapies.

Identifying BBB Penetration and Target Engagement in Molecular and Immunotherapies

Drug delivery, brain penetration, and target engagement are significant limitations in neuro-oncology drug development for both targeted therapies² and immunotherapies³, due in part to the blood-brain barrier (BBB)⁴ and other factors. Depending on the molecular, chemical, and physical characteristics of the therapeutic agent under investigation, it may require transport of the agent via paracellular or transcellular diffusion, carrier- or adsorptive-mediated transport, or receptor-mediated transport⁵. The size of the molecule, charge distribution, and other factors must all be considered when developing agents specific for neuro-oncology⁶, which may explain the large rate of failure of most agents that have been shown to be effective and were designed for other systemic solid tumors⁷.

Evaluation of BBB permeability and initial target engagement for small molecules can be evaluated several ways using advanced imaging techniques early in the drug development process. Dynamic contrast enhanced (DCE) perfusion MRI, a technique utilizing serial T1-weighted MRI during injection of gadolinium-based contrast agents, is often used to quantify exchange of contrast agents between the vascular and extravascular space in a range of diseases⁸. The exchange rate of contrast moving from the vascular to extravascular space, or K^{trans} , has been shown to be dependent on capillary permeability and surface area^{8,9} and can be used as a surrogate of BBB permeability for the purposes of drug development and understanding drug penetration¹⁰. However, the BBB is highly selective, therefore this approach may not reflect BBB permeability to the investigative therapeutic agent, but rather only highlights permeability to the gadolinium-based contrast agent used. An alternative approach may be to radiolabel the investigative agent with a single photon or positron emitting nuclei (e.g. SPECT nuclei ^{99m}Tc or PET nuclei like ¹¹C or ¹⁸F), then evaluate the distribution after infusing this tracer into the patient. For example, Gerstner *et al.*¹¹ investigated drug penetration of temozolomide, an alkylating agent shown to have significant clinical activity in GBM, using radiolabeled [¹¹C]-temozolomide, DCE-MRI, and dynamic susceptibility contrast (DSC) perfusion MRI in recurrent GBM patients treated concurrently with bevacizumab, an anti-angiogenic agent known to reduce BBB permeability. Results from this study showed that in areas where BBB permeability was not compromised on DCE-MRI, increased blood flow on DSC-MRI was sufficient to increase temozolomide uptake within brain tumors. A recent

study by Jucaite *et al.*¹² is another example of this approach being used to successfully determine brain exposure to an experimental therapy. In this study, investigators used microdoses of ¹¹C-AZD1390, a radiolabeled version of a potent and selective ATM inhibitor AZD1390, to measure brain exposure in healthy volunteers and noted the agent crosses the BBB noting that the agent crosses the BBB and has favorable temporal kinetics throughout the brain. This information can be useful for guiding dose ranges and schedules for subsequent clinical studies in order to optimize exposure. This same strategy can be used with most targeted and immunotherapy agents, as many undergo similar early bioavailability, biodistribution, and safety studies using radiolabeled versions of the compound of interest^{13,14}, including peptides and antibodies¹⁵. Radiolabeled versions of common chemotherapies, targeted agents and immunotherapy agents in use today include temozolomide¹¹ (e.g. ¹¹C-temozolomide), lomustine¹⁶ (e.g. ¹⁴C-lomustine), bevacizumab¹⁷ (e.g. ⁸⁹Zr-bevacizumab, ¹¹¹In-bevacizumab, or ¹²⁴I-bevacizumab), cediranib¹⁸ (e.g. ¹⁴C-cediranib), nivolumab^{19,20} (e.g. ⁸⁹Zr-nivolumab, ⁶⁸Ga-nivolumab), and ipilimumab^{21,22} (e.g. ⁶⁴Cu-ipilimumab).

Radiolabeled drugs can provide important information regarding drug penetration and delivery to brain tumors, it does not necessarily address target engagement (Fig. 1). While there are a number of established methods for quantifying target engagement *ex vivo* and *in vivo* within living cells or systems²³⁻²⁶ and temporal characteristics of radiolabeled drug uptake and distribution can be used to infer target engagement using non-labeled drug at increasing concentration to infer receptor characteristics (e.g. ^{27,28}), imaging of direct target engagement remains a significant challenge in human patients²⁹. While still a proof-of-concept, ³¹P-NMR spectroscopic approaches could provide value in understanding phosphorylation of various receptor proteins through the NMR chemical shift of phosphorus nuclei^{30,31}, but this approach has not been shown to be sensitive enough in human brain tumor drug development to date.

Several molecular imaging tracers have also been developed to quantify the presence or activation of T-cell surface markers for immunotherapies in both murine models and humans (reviewed in ³²), including both antibody fragments and cytokines. For example, presence of T-cell receptors (TCR) CD4 and CD8 have been explored using portions of antibodies, or cys-diabodies^{9,33} (e.g. ⁸⁹Zr-malDFO-GK1.5 cDb and ⁸⁹Zr-malDFO-169 cDb, respectively) and minibodies³⁴⁻³⁶ (e.g. ⁸⁹Zr-Df0IAB22M2C). Additionally, strategies to identify target engagement after immunotherapies using the particular activity of the TCR after binding are currently being explored, including the use of human interleukin-2 (IL-2) cytokine tracers (e.g. ^{99m}Tc-HYNIC-IL-2, ¹⁸F-FB-IL-2)³⁷⁻³⁹ and radiolabeled antibodies targeting different TCR domains (e.g. ⁶⁴Cu-cOVA-TCR for quantifying internalization of the TCR-complex⁴⁰ and ⁸⁹Zr-Df-aTCRmu-F(ab')₂ for targeting the beta domain of the TCR⁴¹). In addition to these probes, studies are also exploring the use of PET reporter genes integrated into gene or cell-based immunotherapies^{42,43}.

Using Downstream Biological Effects to Identify Target Engagement in Molecular Therapies

While directly imaging and quantifying target engagement in human patients remains a significant challenge in brain tumor drug development, biological changes that occur downstream from target engagement can provide significant value in early stages of drug development. For example, studies have suggested target engagement in therapies that inhibit mutant IDH enzymes (e.g. “IDH inhibitors”) in IDH mutant cancers results in reduction in 2-hydroxyglutarate (2HG), an oncometabolite detectable using proton MRS that often drives tumorigenesis in these tumors^{44,45}. Similarly, downstream metabolic and physiologic changes that can be quantified using current imaging technologies may provide value following receptor tyrosine kinase (RTK) inhibitors targeting different oncogenic pathways (Fig. 2). For example, PI3K and mTOR activity is known to play an important role in glucose metabolism⁴⁶⁻⁴⁹, thus inhibition of mTOR⁵⁰ or RTK-induced activation of PI3K^{51,52} can be detected using ¹⁸F-FDG PET. PI3K and mTOR activation also influences angiogenesis⁵³ as well as tumor cell proliferation⁵⁴, suggesting techniques like perfusion and diffusion MRI may provide value in determining adequate target engagement through reduction in vascularity⁵⁵⁻⁵⁷ and cellularity⁵⁸⁻⁶³, respectively. As an example of this approach, Ellingson *et al.*⁶⁴ recently used multiparametric MR-PET imaging to explore pharmacokinetics and clinical response to GDC-0084, a brain-penetrant small-molecule inhibitor of PI3K and mTOR. Results from this study showed that composite biomarkers created from ¹⁸F-FDG PET uptake, DCE and DSC perfusion MRI, and diffusion MRI could predict maximum blood concentration, drug exposure, and progression-free survival (PFS) in recurrent GBM treated with GDC-0084, signifying that imaging biomarkers based on downstream effects following target engagement may be useful for early phase drug development studies.

Several non-invasive imaging techniques are available for quantifying these downstream effects beyond those previously mentioned. For example, hyperpolarized ¹³C-glucose or ¹³C-pyruvate MRI/MRS can be used to examine metabolic characteristics including glucose uptake, metabolite generation, and lactate production⁶⁵⁻⁶⁷. Alternatively, investigators recently demonstrated that glucose enhanced MRI can be performed using chemical exchange saturation transfer (CEST) imaging of hydroxyl (-OH) groups on glucose after infusion (glucoCEST)⁶⁸⁻⁷⁰. Lactate production, a product of glycolysis, can also be quantified using either lactate MRS^{71,72} or pH-weighted amine CEST imaging⁷³⁻⁷⁹. For targeted agents that may alter or are influenced by tumor hypoxia⁸⁰, including agents targeting HIF pathways^{81,82}, carbonic anhydrase IX inhibitors⁸³, agents that directly increase oxygenation⁸⁴, or bioreductive prodrugs that become potent in hypoxic environments⁸⁵, the use of ¹⁸F-fluoromisonidazole (¹⁸F-FMISO) PET⁸⁶⁻⁸⁹ or oxygen-sensitive MRI^{79,90} may be useful. For agents that may alter tumor proliferation rate, diffusion MRI⁵⁸⁻⁶³, ¹⁸F-fluorothymidine (¹⁸F-FLT) PET⁹¹⁻⁹³, and amino acid PET (e.g. ¹⁸F-fluorodopa⁶⁰) may be advantageous as surrogates of downstream physiologic changes that can be detected using current imaging technologies.

Using Downstream Biological Effects to Identify Target Engagement in Immunotherapies

After initiation of immunotherapies, several molecular, metabolic, and physiologic changes occur downstream from initial target engagement³². Among these downstream changes are alterations in deoxycytidine kinase (dCK) and deoxyguanosine (dGK) within the deoxyribonucleoside salvage pathway. Among the PET tracers being studied as potential biomarkers for dCK activity are 1-(2'-deoxy-2'-[¹⁸F]fluoroarabinofuranosyl) cytosine⁹⁴ (¹⁸F-FAC) and ¹⁸F-clofarabine⁹⁵⁻⁹⁷ (¹⁸F-CFA), while 2'-deoxy-2'-[¹⁸F]fluoro-9-β-D-arabinofuranosylguanine⁹⁸ (¹⁸F-AraG) is currently being used in a number of clinical trials as a potential biomarker for dGK activity.

In addition to alterations in the deoxyribonucleoside salvage pathway, molecular imaging of amino acid metabolism is another potential useful strategy for using downstream effects to identify target engagement following immunotherapies³². Trans-1-amino-3-[¹⁸F]fluorocyclobutanecarboxylic acid (¹⁸F-FACBC) is currently being studied for use in immunotherapy monitoring and has shown specific uptake in activated immune cells^{99,100}. Other amino acid PET tracers commonly used for neuro oncology^{101,102} also show increased uptake during immunotherapies; however, questions remain as to the specificity of this approach because active tumor also has significant uptake.

Glucose metabolism also appears to be altered in immune cells after activation. Specifically, data suggests elevated glycolytic activity is elevated in GBM exhibiting a favorable immune-stimulatory microenvironment¹⁰³. This suggests that ¹⁸F-FDG PET (and other glycolytic imaging biomarkers including hyperpolarized ¹³C-glucose and glucoCEST) may be useful as a biomarker for immunotherapies¹⁰⁴ as well as molecular or targeted therapies. In solid tumors, data suggests a reduction in ¹⁸F-FDG PET uptake of primary lesions¹⁰⁵ and lack of multiple ¹⁸F-FDG PET avid satellite lesions¹⁰⁶ is suggestive of successful immunotherapy and forms the basis of a new PET Response Evaluation Criteria for Immunotherapy (PERCINT) criteria¹⁰⁴. However, ¹⁸F-FDG PET uptake can be difficult to interpret in brain tumors due to high activity within active tumor from intrinsic glycolytic signaling as well as uptake in normal brain tissue. Additional studies are needed to better understand the benefits and limitations of using ¹⁸F-FDG PET, hyperpolarized ¹³C-glucose/pyruvate, and glucoCEST to monitor immunotherapy response in brain tumors.

Macrophages, including tumor associated macrophages (TAM) that help create an immunosuppressive tumor microenvironment¹⁰⁷⁻¹⁰⁹, utilize iron as a cofactor for a number of functions including energy production, hypoxic regulation, and inflammation¹⁰⁹. Thus, superparamagnetic iron oxide (SPIO) nanoparticles used as contrast agents in MRI may be useful to get a sense of TAM activity within cancers including brain tumors^{110,111}. Data suggests accumulation of SPIOs in macrophages occurs 1-10 days after injection¹¹², meaning a patient would need to be dosed at least 24 hours before the imaging exam. Preclinical evidence suggests solid tumors successfully treated with immunotherapies exhibit a reduction in the measured transverse relaxation time constant (T_2 and T_2^*)^{113,114}, implying a reduction in the concentration of TAMs. This reduction in T_2/T_2^* also appears to result in a reduction in tumor growth rate¹¹⁵, supporting the use of SPIOs to monitor

TAM activity within the tumor. Two commercially available SPIO agents are available for clinical use, ferumoxytol¹¹⁶ (Feraheme, AMAG Pharmaceuticals Inc., Cambridge, MA) and ferucarbotran¹¹⁷ (Resovist, Schering, Berlin, Germany). Ferumoxytol has been used most widely, having the most abundant post-market safety data¹¹² and specifically approved for use in iron replacement therapy, while ferucarbotran was recently approved for use in liver imaging applications but has shown some utility in the CNS¹¹⁸.

Identifying Early Clinical Activity that Increases Likelihood of Meaningful Clinical Outcome

Although overall survival (OS) is the standard for determining treatment efficacy in high grade glioma, early phase clinical trials are typically not powered or designed to identify OS differences. In these early exploratory stages, there could be potential influence of therapies before or after the therapy under investigation. To overcome these limitations and keep study size relatively small, progression-free survival (PFS) and objective response rate (ORR) are considered important end points¹¹⁹. However, PFS and ORR alone suffer from significant limitations, since the natural history and growth rate for some tumors may make landmark PFS targets (e.g. the rate of PFS beyond 6 months from start of treatment, or PFS6) obtainable by chance or not directly attributed to the treatment under investigation. It is possible additional confidence can be gained by clearly understanding the growth trajectory of a tumor before and after initiating a therapy in addition to landmark PFS targets (Fig. 3). Since previous studies show a clear association between tumor size¹²⁰⁻¹²⁹ and growth rates^{120,130-132} with overall survival in GBM, such a framework may be useful for finding clinical activity in early phase trials that increases the likelihood of clinical benefit when advancing to larger and more expensive later stage trials. For example, if a patient has reached the threshold for PFS6 and has a negative or zero (cytostatic) post-treatment growth rate over that period it is more likely that the drug is having meaningful therapeutic activity. If a patient has reached the PFS6 threshold and the tumor growth rate has slowed some, it is possible the drug may be working but there is lower confidence in whether this will translate into meaningful clinical benefit in later stage trials. If a patient reaches the PFS6 threshold but the growth rate after treatment is the same or faster than the pretreatment growth rate, then it is likely the drug is not working. If, on the other hand, a patient does not reach the PFS6 threshold but there is evidence that the drug slowed the tumor growth rate, it is possible there is some therapeutic activity, but the study design or dosing may need to be adjusted in order to translate into clinical benefit. If there is no evidence of extended PFS and tumor growth rate is the same or faster after the treatment, then one can be fairly confident the drug is not working.

Use of the modified response assessment in neuro oncology (mRANO) criteria¹³³ may also be useful to gain additional confidence in PFS measurements (Fig. 4). The mRANO criteria was developed as a treatment agnostic criterion for platform and/or adaptive trials where many types of treatments may be compared. The primary difference between the mRANO criteria¹³³ and the standard RANO criteria¹³⁴ is the requirement for confirmation of progression, essentially merging immunotherapy-specific criteria¹³⁵ with prior guidelines. The mRANO criteria has been successfully used in more than a dozen trials to date as

an operational tool for managing patients on trial. Recent studies¹³⁶ have also shown that the mRANO criteria is feasible in immunotherapy trials and PFS defined using mRANO appears correlated with OS, providing confidence for use of mRANO-defined PFS as a potential surrogate for clinical benefit in high grade gliomas.

According to the mRANO criteria, if a patient has no measurable enhancing disease at baseline, then the best response they can obtain is stable disease (SD). However, if enhancing disease becomes measurable in these patients after starting treatment, meaning larger than 1cm x 1cm perpendicular dimensions on at least two slices, then the patient is said to have “preliminary progressive disease (PD)”, and the patient should continue on treatment (if possible) until progression can be confirmed at the next follow up time point. If a patient has measurable disease at baseline, which is mostly the case in studies involving recurrent disease, and after the first post-treatment scan there is no measurable enhancing disease, the patient is said to have “preliminary complete response (CR)”, which then needs to be confirmed at the next time point. If at this next time point ($n+1$) there is no measurable enhancing or non-enhancing disease, CR is confirmed and the patient stays on treatment until another event occurs. If the patient has non-measurable disease but no enhancing disease, then the patient has a “confirmed partial response (PR)”, and the patient continues on treatment. If the patient has emergence of measurable enhancing disease, then this constitutes preliminary PD and the patient continues on treatment (if possible) until progression can be confirmed at the next follow up time point.

If a patient has measurable disease at baseline and a time point after treatment (n) the lesion shrinks more than 50% from baseline, then the patient has “preliminary partial response (PR)” and the patient continues therapy until the next time point ($n+1$). If at this time point there is no measurable enhancing disease, this patient has a confirmed PR, but preliminary CR and should continue treatment to see if the preliminary CR can be confirmed at the next follow up time point. Alternatively, if at the confirmation time point ($n+1$) there remains measurable disease and it is still less than 50% from baseline, this is determined to be a sustained, or confirmed PR and the patient should continue treatment until disease progression is identified. If the lesion is not confirmed to be more than 50% smaller than the baseline and is instead more than 25% *larger* than the nadir (n) time point, then this constitutes preliminary PD and the patient should continue on therapy until PD can be confirmed at the next time point. If instead the lesion has not grown more than 25% from the nadir but is not 50% smaller than baseline, this constitutes stable disease (and a non-sustained, non-confirmed PR) and the patient should continue treatment until disease progression has been identified and confirmed if possible.

If the patient at any time has a growing lesion that is more than 25% with respect to the nadir, this will constitute preliminary PD and the patient should continue treatment until this can be confirmed at the subsequent time point ($n+1$). If at this confirmation time point ($n+1$) the lesion has continued to grow more than 25% from the previous preliminary PD time point (n), then this is confirmed PD and the date of progression is at time (n). If instead the lesion has not continued to grow or doesn't meet the 25% threshold for confirmation, then this constitutes “confirmed pseudoprogression (PsP)” and stable disease (SD), since it is presumed the lesion has either slowed growth, stabilized, or shrunk with respect to the

preliminary PD time point. If PsP is confirmed, then the patient should continue therapy until PD can be confirmed at a later time point (m). If at this later time point (m) the patient has an event in which there is 25% growth with respect to either time point (n), where initial progression was noted, or nadir *after* PsP at time point (n), then this constitutes confirmation of PD and the date of progression is time (m). If the patient continues to not reach this 25% threshold with respect to either time point (n) or nadir *after* PsP at time point (n), then this constitutes stable disease (SD) and the patient should continue on treatment until a 2nd PD event is identified.

In summary, the use of advanced imaging technology can provide a wealth of important information about therapeutic response assessment for both molecular and immunotherapies. These approaches can be tailored to the specific agents being tested and the relevant clinical questions depending on the stage of drug development, ranging from verifying that drug is getting into the brain and hitting the desired target through confirming tumor shrinkage that will increase confidence of a clinical benefit in later stages of testing.

Funding:

Funding was provided by the American Cancer Society (ACS) Research Scholar Grant (RSG-15-003-01-CCE) (Ellingson), UCLA SPORE in Brain Cancer (NIH/NCI P50 CA211015) (Ellingson), the Harvard SPORE in Brain Cancer (NIH/NCI P50 CA165962) and NIH/NCI R21 CA223757 (Ellingson).

References

1. Wen PY, Weller M, Lee EQ, et al. Glioblastoma in adults: a Society for Neuro-Oncology (SNO) and European Society of Neuro-Oncology (EANO) consensus review on current management and future directions. *Neuro-oncology* 2020;22:1073–113. [PubMed: 32328653]
2. Shergalis A, Bankhead A 3rd, Luesakul U, Muangsin N, Neamati N. Current Challenges and Opportunities in Treating Glioblastoma. *Pharmacol Rev* 2018;70:412–45. [PubMed: 29669750]
3. Chuntova P, Chow F, Watchmaker PB, et al. Unique challenges for glioblastoma immunotherapy—discussions across neuro-oncology and non-neuro-oncology experts in cancer immunology. Meeting Report from the 2019 SNO Immuno-Oncology Think Tank. *Neuro Oncol* 2021;23:356–75. [PubMed: 33367885]
4. Arvanitis CD, Ferraro GB, Jain RK. The blood–brain barrier and blood–tumour barrier in brain tumours and metastases. *Nature Reviews Cancer* 2020;20:26–41. [PubMed: 31601988]
5. Wong KH, Riaz MK, Xie Y, et al. Review of Current Strategies for Delivering Alzheimer's Disease Drugs across the Blood-Brain Barrier. *Int J Mol Sci* 2019;20:381.
6. Laquintana V, Trapani A, Denora N, Wang F, Gallo JM, Trapani G. New strategies to deliver anticancer drugs to brain tumors. *Expert Opin Drug Deliv* 2009;6:1017–32. [PubMed: 19732031]
7. Levin VA. Drug discovery in neuro-oncology: challenges in the path forward. *Neuro-Oncology* 2018;20:435–6. [PubMed: 29538691]
8. Tofts PS, Brix G, Buckley DL, et al. Estimating kinetic parameters from dynamic contrast-enhanced T(1)-weighted MRI of a diffusible tracer: standardized quantities and symbols. *J Magn Reson Imaging* 1999;10:223–32. [PubMed: 10508281]
9. Freise AC, Zettlitz KA, Salazar FB, Lu X, Tavaré R, Wu AM. ImmunoPET Imaging of Murine CD4(+) T Cells Using Anti-CD4 Cys-Diabody: Effects of Protein Dose on T Cell Function and Imaging. *Mol Imaging Biol* 2017;19:599–609. [PubMed: 27966069]
10. Levin VA, Ellingson BM. Understanding brain penetrance of anticancer drugs. *Neuro-Oncology* 2018;20:589–96. [PubMed: 29474640]

11. Gerstner ER, Emblem KE, Chang K, et al. Bevacizumab Reduces Permeability and Concurrent Temozolomide Delivery in a Subset of Patients with Recurrent Glioblastoma. *Clin Cancer Res* 2020;26:206–12. [PubMed: 31558474]
12. Jucaite A, Stenkrona P, Cselényi Z, et al. Brain exposure of the ATM inhibitor AZD1390 in humans—a positron emission tomography study. *Neuro-oncology* 2021;23:687–96. [PubMed: 33123736]
13. Lamb J, Holland JP. Advanced Methods for Radiolabeling Multimodality Nanomedicines for SPECT/MRI and PET/MRI. *J Nucl Med* 2018;59:382–9. [PubMed: 29025988]
14. Massoud TF, Gambhir SS. Molecular imaging in living subjects: seeing fundamental biological processes in a new light. *Genes Dev* 2003;17:545–80. [PubMed: 12629038]
15. Krzyszczyk P, Czarnecka K, Królicki L, Mikiciuk-Olasik E, Szymański P. Radiolabeled Peptides and Antibodies in Medicine. *Bioconjugate Chemistry* 2021;32:25–42. [PubMed: 33325685]
16. Litterst CL, Mimnaugh EG, Cowles AC, Gram TE, Guarino AM. Distribution of ¹⁴C-Lomustine (¹⁴C-CCNU)-Derived Radioactivity following Intravenous Administration of Three Potential Clinical Formulations to Rabbits. *Journal of Pharmaceutical Sciences* 1974;63:1718–21. [PubMed: 4427229]
17. Nagengast WB, de Vries EG, Hospers GA, et al. In vivo VEGF imaging with radiolabeled bevacizumab in a human ovarian tumor xenograft. *J Nucl Med* 2007;48:1313–9. [PubMed: 17631557]
18. Schulz-Utermoehl T, Spear M, Pollard CRJ, et al. In Vitro Hepatic Metabolism of Cediranib, a Potent Vascular Endothelial Growth Factor Tyrosine Kinase Inhibitor: Interspecies Comparison and Human Enzymology. *Drug Metabolism and Disposition* 2010;38:1688–97. [PubMed: 20634336]
19. England CG, Jiang D, Ehlerding EB, et al. ⁸⁹Zr-labeled nivolumab for imaging of T-cell infiltration in a humanized murine model of lung cancer. *Eur J Nucl Med Mol Imaging* 2018;45:110–20. [PubMed: 28821924]
20. Niemeijer AN, Leung D, Huisman MC, et al. Whole body PD-1 and PD-L1 positron emission tomography in patients with non-small-cell lung cancer. *Nature Communications* 2018;9:4664.
21. Ehlerding EB, Lee HJ, Jiang D, et al. Antibody and fragment-based PET imaging of CTLA-4+ T-cells in humanized mouse models. *Am J Cancer Res* 2019;9:53–63. [PubMed: 30755811]
22. Higashikawa K, Yagi K, Watanabe K, et al. ⁶⁴Cu-DOTA-anti-CTLA-4 mAb enabled PET visualization of CTLA-4 on the T-cell infiltrating tumor tissues. *PLoS One* 2014;9:e109866. [PubMed: 25365349]
23. Simon GM, Niphakis MJ, Cravatt BF. Determining target engagement in living systems. *Nat Chem Biol* 2013;9:200–5. [PubMed: 23508173]
24. Martinez Molina D, Jafari R, Ignatushchenko M, et al. Monitoring drug target engagement in cells and tissues using the cellular thermal shift assay. *Science* 2013;341:84–7. [PubMed: 23828940]
25. Savitski MM, Reinhard FB, Franken H, et al. Tracking cancer drugs in living cells by thermal profiling of the proteome. *Science* 2014;346:1255784. [PubMed: 25278616]
26. Martinez Molina D, Nordlund P. The Cellular Thermal Shift Assay: A Novel Biophysical Assay for In Situ Drug Target Engagement and Mechanistic Biomarker Studies. *Annu Rev Pharmacol Toxicol* 2016;56:141–61. [PubMed: 26566155]
27. Menke-van der Houvenvan Oordt CW, McGeoch A, Bergstrom M, et al. Immuno-PET Imaging to Assess Target Engagement: Experience from ⁸⁹Zr-Anti-HER3 mAb (GSK2849330) in Patients with Solid Tumors. *J Nucl Med* 2019;60:902–9. [PubMed: 30733323]
28. Henry KE, Dacek MM, Dilling TR, et al. A PET Imaging Strategy for Interrogating Target Engagement and Oncogene Status in Pancreatic Cancer. *Clinical cancer research : an official journal of the American Association for Cancer Research* 2019;25:166–76. [PubMed: 30228208]
29. Maynard J, Hart P. The Opportunities and Use of Imaging to Measure Target Engagement. *SLAS Discov* 2020;25:127–36. [PubMed: 31885303]
30. Hirai H, Yoshioka K, Yamada K. A simple method using ³¹P-NMR spectroscopy for the study of protein phosphorylation. *Brain Res Brain Res Protoc* 2000;5:182–9. [PubMed: 10775839]
31. Siegal G, Selenko P. Cells, drugs and NMR. *Journal of Magnetic Resonance* 2019;306:202–12. [PubMed: 31358370]

32. Krekorian M, Fruhwirth GO, Srinivas M, et al. Imaging of T-cells and their responses during anti-cancer immunotherapy. *Theranostics*2019;9:7924–47. [PubMed: 31656546]
33. Tavaré R, Escuin-Ordinas H, Mok S, et al. An Effective Immuno-PET Imaging Method to Monitor CD8-Dependent Responses to Immunotherapy. *Cancer Res*2016;76:73–82. [PubMed: 26573799]
34. Pandit-Taskar N, Postow MA, Hellmann MD, et al. First-in-Humans Imaging with (89)Zr-Df-IAB22M2C Anti-CD8 Minibody in Patients with Solid Malignancies: Preliminary Pharmacokinetics, Biodistribution, and Lesion Targeting. *J Nucl Med*2020;61:512–9. [PubMed: 31586002]
35. Griessinger CM, Olafsen T, Mascioni A, et al. The PET-Tracer ⁸⁹Zr-Df-IAB22M2C Enables Monitoring of Intratumoral CD8 T-cell Infiltrates in Tumor-Bearing Humanized Mice after T-cell Bispecific Antibody Treatment. *Cancer Research*2020;80:2903–13. [PubMed: 32409308]
36. Postow MA, Harding JJ, Hellmann MD, et al. Imaging of tumor infiltrating T cells with an anti-CD8 minibody (Mb) ⁸⁹Zr-IAB22M2C, in advanced solid tumors. *Journal of Clinical Oncology*2018;36:e24160–e.
37. Markovic SN, Galli F, Suman VJ, et al. Non-invasive visualization of tumor infiltrating lymphocytes in patients with metastatic melanoma undergoing immune checkpoint inhibitor therapy: a pilot study. *Oncotarget*2018;9:30268–78. [PubMed: 30100988]
38. Hartimath SV, Draghiciu O, van de Wall S, et al. Noninvasive monitoring of cancer therapy induced activated T cells using [(18)F]FB-IL-2 PET imaging. *Oncoimmunology*2016;6:e1248014–e. [PubMed: 28197364]
39. Shaker MA, Younes HM. Interleukin-2: evaluation of routes of administration and current delivery systems in cancer therapy. *J Pharm Sci*2009;98:2268–98. [PubMed: 19009549]
40. Griessinger CM, Maurer A, Kesenheimer C, et al. ⁶⁴Cu antibody-targeting of the T-cell receptor and subsequent internalization enables in vivo tracking of lymphocytes by PET. *Proc Natl Acad Sci U S A*2015;112:1161–6. [PubMed: 25587131]
41. Mayer KE, Mall S, Yusufi N, et al. T-cell functionality testing is highly relevant to developing novel immuno-tracers monitoring T cells in the context of immunotherapies and revealed CD7 as an attractive target. *Theranostics*2018;8:6070–87. [PubMed: 30613283]
42. Martinez O, Sosabowski J, Maher J, Papa S. New Developments in Imaging Cell-Based Therapy. *J Nucl Med*2019;60:730–5. [PubMed: 30979822]
43. Moroz MA, Zhang H, Lee J, et al. Comparative Analysis of T Cell Imaging with Human Nuclear Reporter Genes. *J Nucl Med*2015;56:1055–60. [PubMed: 26025962]
44. Batsios G, Viswanath P, Subramani E, et al. PI3K/mTOR inhibition of IDH1 mutant glioma leads to reduced 2HG production that is associated with increased survival. *Sci Rep*2019;9:10521. [PubMed: 31324855]
45. Suh CH, Kim HS, Jung SC, Choi CG, Kim SJ. 2-Hydroxyglutarate MR spectroscopy for prediction of isocitrate dehydrogenase mutant glioma: a systemic review and meta-analysis using individual patient data. *Neuro Oncol*2018;20:1573–83. [PubMed: 30020513]
46. Sharma S, Guthrie PH, Chan SS, Haq S, Taegtmeier H. Glucose phosphorylation is required for insulin-dependent mTOR signalling in the heart. *Cardiovasc Res*2007;76:71–80. [PubMed: 17553476]
47. Fuchs BC, Finger RE, Onan MC, Bode BP. ASCT2 silencing regulates mammalian target-of-rapamycin growth and survival signaling in human hepatoma cells. *Am J Physiol Cell Physiol*2007;293:C55–63. [PubMed: 17329400]
48. Kimball SR, Jefferson LS. Signaling pathways and molecular mechanisms through which branched-chain amino acids mediate translational control of protein synthesis. *J Nutr*2006;136:227s–31s. [PubMed: 16365087]
49. Raught B, Gingras A-C, Sonenberg N. The target of rapamycin (TOR) proteins. *Proceedings of the National Academy of Sciences*2001;98:7037–44.
50. Wei LH, Su H, Hildebrandt IJ, Phelps ME, Czernin J, Weber WA. Changes in tumor metabolism as readout for Mammalian target of rapamycin kinase inhibition by rapamycin in glioblastoma. *Clin Cancer Res*2008;14:3416–26. [PubMed: 18519772]
51. De Rosa V, Iommelli F, Monti M, Mainolfi CG, Fonti R, Del Vecchio S. Early (18)F-FDG uptake as a reliable imaging biomarker of T790M-mediated resistance but not MET amplification in

- non-small cell lung cancer treated with EGFR tyrosine kinase inhibitors. *EJNMMI Res*2016;6:74-. [PubMed: 27726115]
52. Su H, Bodenstern C, Dumont RA, et al. Monitoring tumor glucose utilization by positron emission tomography for the prediction of treatment response to epidermal growth factor receptor kinase inhibitors. *Clin Cancer Res*2006;12:5659–67. [PubMed: 17020967]
 53. Karar J, Maity A. PI3K/AKT/mTOR Pathway in Angiogenesis. *Front Mol Neurosci*2011;4:51. [PubMed: 22144946]
 54. Janku F, Yap TA, Meric-Bernstam F. Targeting the PI3K pathway in cancer: are we making headway? *Nat Rev Clin Oncol*2018;15:273–91. [PubMed: 29508857]
 55. Dennie J, Mandeville JB, Boxerman JL, Packard SD, Rosen BR, Weisskoff RM. NMR imaging of changes in vascular morphology due to tumor angiogenesis. *Magn Reson Med*1998;40:793–9. [PubMed: 9840821]
 56. Kellner E, Breyer T, Gall P, et al. MR evaluation of vessel size imaging of human gliomas: Validation by histopathology. *J Magn Reson Imaging*2015;42:1117–25. [PubMed: 25683112]
 57. Chakhoyan A, Yao J, Leu K, et al. Validation of vessel size imaging (VSI) in high-grade human gliomas using magnetic resonance imaging, image-guided biopsies, and quantitative immunohistochemistry. *Scientific Reports*2019;9:2846. [PubMed: 30808879]
 58. Sugahara T, Korogi Y, Kochi M, et al. Usefulness of diffusion-weighted MRI with echo-planar technique in the evaluation of cellularity in gliomas. *J Magn Reson Imaging*1999;9:53–60. [PubMed: 10030650]
 59. Ellingson BM, Malkin MG, Rand SD, et al. Validation of functional diffusion maps (fDMs) as a biomarker for human glioma cellularity. *J Magn Reson Imaging*2010;31:538–48. [PubMed: 20187195]
 60. Karavaeva E, Harris RJ, Leu K, et al. Relationship Between [18F]FDOPA PET Uptake, Apparent Diffusion Coefficient (ADC), and Proliferation Rate in Recurrent Malignant Gliomas. *Mol Imaging Biol*2015;17:434–42. [PubMed: 25465392]
 61. Chenevert TL, Stegman LD, Taylor JM, et al. Diffusion magnetic resonance imaging: an early surrogate marker of therapeutic efficacy in brain tumors. *Journal of the National Cancer Institute*2000;92:2029–36. [PubMed: 11121466]
 62. Gupta RK, Cloughesy TF, Sinha U, et al. Relationships between choline magnetic resonance spectroscopy, apparent diffusion coefficient and quantitative histopathology in human glioma. *J Neurooncol*2000;50:215–26. [PubMed: 11263501]
 63. Lyng H, Haraldseth O, Rofstad EK. Measurement of cell density and necrotic fraction in human melanoma xenografts by diffusion weighted magnetic resonance imaging. *Magn Reson Med*2000;43:828–36. [PubMed: 10861877]
 64. Ellingson BM, Yao J, Raymond C, et al. Multiparametric MR-PET Imaging Predicts Pharmacokinetics and Clinical Response to GDC-0084 in Patients with Recurrent High-Grade Glioma. *Clin Cancer Res*2020;26:3135–44. [PubMed: 32269051]
 65. Mishkovsky M, Gussyatiner O, Lanz B, et al. Hyperpolarized ¹³C-glucose magnetic resonance highlights reduced aerobic glycolysis in vivo in infiltrative glioblastoma. *Scientific Reports*2021;11:5771. [PubMed: 33707647]
 66. Chen J, Patel TR, Pinho MC, et al. Preoperative Imaging of Glioblastoma Patients using Hyperpolarized ¹³C Pyruvate: Potential Role in Clinical Decision Making. *Neuro-Oncology Advances*2021.
 67. Najac C, Ronen SM. MR Molecular Imaging of Brain Cancer Metabolism Using Hyperpolarized ¹³C Magnetic Resonance Spectroscopy. *Top Magn Reson Imaging*2016;25:187–96. [PubMed: 27748711]
 68. Xu X, Yadav NN, Knutsson L, et al. Dynamic Glucose-Enhanced (DGE) MRI: Translation to Human Scanning and First Results in Glioma Patients. *Tomography*2015;1:105–14. [PubMed: 26779568]
 69. Xu X, Xu J, Knutsson L, et al. The effect of the mTOR inhibitor rapamycin on glucoCEST signal in a preclinical model of glioblastoma. *Magn Reson Med*2019;81:3798–807. [PubMed: 30793789]
 70. Paech D, Schuenke P, Koehler C, et al. T1ρ-weighted Dynamic Glucose-enhanced MR Imaging in the Human Brain. *Radiology*2017;285:914–22. [PubMed: 28628422]

71. Nakamura H, Doi M, Suzuki T, et al. The Significance of Lactate and Lipid Peaks for Predicting Primary Neuroepithelial Tumor Grade with Proton MR Spectroscopy. *Magn Reson Med* 2018;17:238–43. [PubMed: 28819084]
72. Bisdas S, Schäfer R, Kolb R, Bender B, Klose U. Lactate as clinical tumour biomarker: Optimization of lactate detection and quantification in MR spectroscopic imaging of glioblastomas. *European Journal of Radiology* 2020;130:109171. [PubMed: 32668356]
73. Wang YL, Yao J, Chakhoyan A, et al. Association between Tumor Acidity and Hypervascularity in Human Gliomas Using pH-Weighted Amine Chemical Exchange Saturation Transfer Echo-Planar Imaging and Dynamic Susceptibility Contrast Perfusion MRI at 3T. *AJNR Am J Neuroradiol* 2019;40:979–86. [PubMed: 31097430]
74. Yao J, Chakhoyan A, Nathanson DA, et al. Metabolic characterization of human IDH mutant and wild type gliomas using simultaneous pH- and oxygen-sensitive molecular MRI. *Neuro Oncol* 2019;21:1184–96. [PubMed: 31066901]
75. Yao J, Ruan D, Raymond C, et al. Improving B0 Correction for pH-Weighted Amine Proton Chemical Exchange Saturation Transfer (CEST) Imaging by Use of k-Means Clustering and Lorentzian Estimation. *Tomography* 2018;4:123–37. [PubMed: 30320212]
76. Yao J, Tan CHP, Schlossman J, et al. pH-weighted amine chemical exchange saturation transfer echoplanar imaging (CEST-EPI) as a potential early biomarker for bevacizumab failure in recurrent glioblastoma. *J Neurooncol* 2019;142:587–95. [PubMed: 30806888]
77. Harris RJ, Cloughesy TF, Liau LM, et al. Simulation, phantom validation, and clinical evaluation of fast pH-weighted molecular imaging using amine chemical exchange saturation transfer echo planar imaging (CEST-EPI) in glioma at 3 T. *NMR Biomed* 2016;29:1563–76. [PubMed: 27717216]
78. Harris RJ, Cloughesy TF, Liau LM, et al. pH-weighted molecular imaging of gliomas using amine chemical exchange saturation transfer MRI. *Neuro Oncol* 2015;17:1514–24. [PubMed: 26113557]
79. Harris RJ, Yao J, Chakhoyan A, et al. Simultaneous pH-sensitive and oxygen-sensitive MRI of human gliomas at 3 T using multi-echo amine proton chemical exchange saturation transfer spin-and-gradient echo echo-planar imaging (CEST-SAGE-EPI). *Magn Reson Med* 2018;80:1962–78. [PubMed: 29626359]
80. Skwarski M, Bowler E, Wilson JD, Higgins GS, Hammond EM. Targeting Tumor Hypoxia. In: Willers H, Eke I, eds. *Molecular Targeted Radiosensitizers: Opportunities and Challenges*. Cham: Springer International Publishing; 2020:265–99.
81. Rapisarda A, Uranchimeg B, Scudiero DA, et al. Identification of small molecule inhibitors of hypoxia-inducible factor 1 transcriptional activation pathway. *Cancer Res* 2002;62:4316–24. [PubMed: 12154035]
82. Kaur B, Khwaja FW, Severson EA, Matheny SL, Brat DJ, Van Meir EG. Hypoxia and the hypoxia-inducible-factor pathway in glioma growth and angiogenesis. *Neuro Oncol* 2005;7:134–53. [PubMed: 15831232]
83. Lou Y, McDonald PC, Oloumi A, et al. Targeting tumor hypoxia: suppression of breast tumor growth and metastasis by novel carbonic anhydrase IX inhibitors. *Cancer Res* 2011;71:3364–76. [PubMed: 21415165]
84. Siemann DW, Horsman MR. Modulation of the tumor vasculature and oxygenation to improve therapy. *Pharmacol Ther* 2015;153:107–24. [PubMed: 26073310]
85. Guise CP, Mowday AM, Ashoorzadeh A, et al. Bioreductive prodrugs as cancer therapeutics: targeting tumor hypoxia. *Chin J Cancer* 2014;33:80–6. [PubMed: 23845143]
86. Gerstner ER, Zhang Z, Fink JR, et al. ACRIN 6684: Assessment of Tumor Hypoxia in Newly Diagnosed Glioblastoma Using 18F-FMISO PET and MRI. *Clin Cancer Res* 2016;22:5079–86. [PubMed: 27185374]
87. Abdo RA, Lamare F, Fernandez P, Bentourkia M. Analysis of hypoxia in human glioblastoma tumors with dynamic 18F-FMISO PET imaging. *Australas Phys Eng Sci Med* 2019;42:981–93. [PubMed: 31520369]
88. Kobayashi H, Hirata K, Yamaguchi S, Terasaka S, Shiga T, Houkin K. Usefulness of FMISO-PET for glioma analysis. *Neurol Med Chir (Tokyo)* 2013;53:773–8. [PubMed: 24172591]

89. Bekaert L, Valable S, Lechapt-Zalcman E, et al. [18F]-FMISO PET study of hypoxia in gliomas before surgery: correlation with molecular markers of hypoxia and angiogenesis. *Eur J Nucl Med Mol Imaging*2017;44:1383–92. [PubMed: 28315948]
90. Oughourlian TC, Yao J, Hagiwara A, et al. Relative oxygen extraction fraction (rOEF) MR imaging reveals higher hypoxia in human epidermal growth factor receptor (EGFR) amplified compared with non-amplified gliomas. *Neuroradiology*2021;63:857–68. [PubMed: 33106922]
91. Been LB, Suurmeijer AJ, Cobben DC, Jager PL, Hoekstra HJ, Elsinga PH. [18F]FLT-PET in oncology: current status and opportunities. *Eur J Nucl Med Mol Imaging*2004;31:1659–72. [PubMed: 15565331]
92. McKinley ET, Ayers GD, Smith RA, et al. Limits of [18F]-FLT PET as a biomarker of proliferation in oncology. *PLoS One*2013;8:e58938. [PubMed: 23554961]
93. Bollineni VR, Kramer GM, Jansma EP, Liu Y, Oyen WJG. A systematic review on [18F]FLT-PET uptake as a measure of treatment response in cancer patients. *European Journal of Cancer*2016;55:81–97. [PubMed: 26820682]
94. Radu CG, Shu CJ, Nair-Gill E, et al. Molecular imaging of lymphoid organs and immune activation by positron emission tomography with a new [18F]-labeled 2'-deoxycytidine analog. *Nat Med*2008;14:783–8. [PubMed: 18542051]
95. Kim W, Le TM, Wei L, et al. [18F]CFA as a clinically translatable probe for PET imaging of deoxycytidine kinase activity. *Proc Natl Acad Sci U S A*2016;113:4027–32. [PubMed: 27035974]
96. Barrio MJ, Spick C, Radu CG, et al. Human Biodistribution and Radiation Dosimetry of (18)F-Clofarabine, a PET Probe Targeting the Deoxyribonucleoside Salvage Pathway. *J Nucl Med*2017;58:374–8. [PubMed: 27811125]
97. Antonios JP, Soto H, Everson RG, et al. Detection of immune responses after immunotherapy in glioblastoma using PET and MRI. *Proceedings of the National Academy of Sciences*2017;114:10220–5.
98. Ronald JA, Kim BS, Gowrishankar G, et al. A PET Imaging Strategy to Visualize Activated T Cells in Acute Graft-versus-Host Disease Elicited by Allogeneic Hematopoietic Cell Transplant. *Cancer Res*2017;77:2893–902. [PubMed: 28572504]
99. Kanagawa M, Doi Y, Oka S, et al. Comparison of trans-1-amino-3-[18F]fluorocyclobutanecarboxylic acid (anti-[18F]FACBC) accumulation in lymph node prostate cancer metastasis and lymphadenitis in rats. *Nucl Med Biol*2014;41:545–51. [PubMed: 24816330]
100. Oka S, Okudaira H, Ono M, et al. Differences in transport mechanisms of trans-1-amino-3-[18F]fluorocyclobutanecarboxylic acid in inflammation, prostate cancer, and glioma cells: comparison with L-[methyl-11C]methionine and 2-deoxy-2-[18F]fluoro-D-glucose. *Mol Imaging Biol*2014;16:322–9. [PubMed: 24136390]
101. Najjar AM, Johnson JM, Schellingerhout D. The Emerging Role of Amino Acid PET in Neuro-Oncology. *Bioengineering (Basel)*2018;5.
102. Albert NL, Weller M, Suchorska B, et al. Response Assessment in Neuro-Oncology working group and European Association for Neuro-Oncology recommendations for the clinical use of PET imaging in gliomas. *Neuro-Oncology*2016;18:1199–208. [PubMed: 27106405]
103. Jiang Z, Liu Z, Li M, Chen C, Wang X. Increased glycolysis correlates with elevated immune activity in tumor immune microenvironment. *EBioMedicine*2019;42:431–42. [PubMed: 30935888]
104. Aide N, Hicks RJ, Le Tourneau C, Lheureux S, Fanti S, Lopci E. FDG PET/CT for assessing tumour response to immunotherapy : Report on the EANM symposium on immune modulation and recent review of the literature. *Eur J Nucl Med Mol Imaging*2019;46:238–50. [PubMed: 30291373]
105. Sachpekidis C, Anwar H, Winkler J, et al. The role of interim (18)F-FDG PET/CT in prediction of response to ipilimumab treatment in metastatic melanoma. *Eur J Nucl Med Mol Imaging*2018;45:1289–96. [PubMed: 29478079]
106. Anwar H, Sachpekidis C, Winkler J, et al. Absolute number of new lesions on (18)F-FDG PET/CT is more predictive of clinical response than SUV changes in metastatic melanoma patients receiving ipilimumab. *Eur J Nucl Med Mol Imaging*2018;45:376–83. [PubMed: 29124281]

107. Liu T, Larionova I, Litviakov N, et al. Tumor-associated macrophages in human breast cancer produce new monocyte attracting and pro-angiogenic factor YKL-39 indicative for increased metastasis after neoadjuvant chemotherapy. *Oncoimmunology* 2018;7:e1436922–e. [PubMed: 29872578]
108. Zhou J, Tang Z, Gao S, Li C, Feng Y, Zhou X. Tumor-Associated Macrophages: Recent Insights and Therapies. *Frontiers in Oncology* 2020;10.
109. Nemeth E, Ganz T. Regulation of iron metabolism by hepcidin. *Annu Rev Nutr* 2006;26:323–42. [PubMed: 16848710]
110. Yang R, Sarkar S, Yong VW, Dunn JF. In Vivo MR Imaging of Tumor-Associated Macrophages: The Next Frontier in Cancer Imaging. *Magn Reson Insights* 2018;11:1178623x18771974.
111. Li K, Nejadnik H, Daldrup-Link HE. Next-generation superparamagnetic iron oxide nanoparticles for cancer theranostics. *Drug Discov Today* 2017;22:1421–9. [PubMed: 28454771]
112. Nguyen K-L, Yoshida T, Kathuria-Prakash N, et al. Multicenter Safety and Practice for Off-Label Diagnostic Use of Ferumoxytol in MRI. *Radiology* 2019;293:554–64. [PubMed: 31638489]
113. Mohanty S, Yerneni K, Theruvath JL, et al. Nanoparticle enhanced MRI can monitor macrophage response to CD47 mAb immunotherapy in osteosarcoma. *Cell Death & Disease* 2019;10:36. [PubMed: 30674867]
114. Daldrup-Link HE, Golovko D, Ruffell B, et al. MRI of tumor-associated macrophages with clinically applicable iron oxide nanoparticles. *Clin Cancer Res* 2011;17:5695–704. [PubMed: 21791632]
115. Mukherjee S, Sonanini D, Maurer A, Daldrup-Link HE. The yin and yang of imaging tumor associated macrophages with PET and MRI. *Theranostics* 2019;9:7730–48. [PubMed: 31695797]
116. Toth GB, Varallyay CG, Horvath A, et al. Current and potential imaging applications of ferumoxytol for magnetic resonance imaging. *Kidney International* 2017;92:47–66. [PubMed: 28434822]
117. Reimer P, Balzer T. Ferucarbotran (Resovist): a new clinically approved RES-specific contrast agent for contrast-enhanced MRI of the liver: properties, clinical development, and applications. *Eur Radiol* 2003;13:1266–76. [PubMed: 12764641]
118. Bendszus M, Stoll G. Caught in the Act: *In Vivo* Mapping of Macrophage Infiltration in Nerve Injury by Magnetic Resonance Imaging. *The Journal of Neuroscience* 2003;23:10892–6. [PubMed: 14645484]
119. Lamborn KR, Yung WK, Chang SM, et al. Progression-free survival: an important end point in evaluating therapy for recurrent high-grade gliomas. *Neuro Oncol* 2008;10:162–70. [PubMed: 18356283]
120. Ellingson BM, Wen PY, Cloughesy TF. Evidence and context of use for contrast enhancement as a surrogate of disease burden and treatment response in malignant glioma. *Neuro Oncol* 2018;20:457–71. [PubMed: 29040703]
121. Wood JR, Green SB, Shapiro WR. The prognostic importance of tumor size in malignant gliomas: a computed tomographic scan study by the Brain Tumor Cooperative Group. *J Clin Oncol* 1988;6:338–43. [PubMed: 3339397]
122. Curran WJ Jr., Scott CB, Horton J, et al. Recursive partitioning analysis of prognostic factors in three Radiation Therapy Oncology Group malignant glioma trials. *Journal of the National Cancer Institute* 1993;85:704–10. [PubMed: 8478956]
123. McGirt MJ, Chaichana KL, Gathinji M, et al. Independent association of extent of resection with survival in patients with malignant brain astrocytoma. *Journal of neurosurgery* 2009;110:156–62. [PubMed: 18847342]
124. Bauchet L, Mathieu-Daude H, Fabbro-Peray P, et al. Oncological patterns of care and outcome for 952 patients with newly diagnosed glioblastoma in 2004. *Neuro Oncol* 2010;12:725–35. [PubMed: 20364023]
125. Zinn PO, Coleen RR, Kasper EM, Burkhardt JK. Extent of resection and radiotherapy in GBM: A 1973 to 2007 surveillance, epidemiology and end results analysis of 21,783 patients. *International journal of oncology* 2013;42:929–34. [PubMed: 23338774]

126. Pan IW, Ferguson SD, Lam S. Patient and treatment factors associated with survival among adult glioblastoma patients: A USA population-based study from 2000-2010. *Journal of clinical neuroscience : official journal of the Neurosurgical Society of Australasia*2015.
127. Ellingson BM, Kim E, Woodworth DC, et al. Diffusion MRI quality control and functional diffusion map results in ACRIN 6677/RTOG 0625: a multicenter, randomized, phase II trial of bevacizumab and chemotherapy in recurrent glioblastoma. *International journal of oncology*2015;46:1883–92. [PubMed: 25672376]
128. Ellingson BM, Kim HJ, Woodworth DC, et al. Recurrent glioblastoma treated with bevacizumab: contrast-enhanced T1-weighted subtraction maps improve tumor delineation and aid prediction of survival in a multicenter clinical trial. *Radiology*2014;271:200–10. [PubMed: 24475840]
129. Ellingson BM, Harris RJ, Woodworth DC, et al. Baseline pretreatment contrast enhancing tumor volume including central necrosis is a prognostic factor in recurrent glioblastoma: evidence from single and multicenter trials. *Neuro Oncol*2017;19:89–98. [PubMed: 27580889]
130. Smedley NF, Ellingson BM, Cloughesy TF, Hsu W. Longitudinal Patterns in Clinical and Imaging Measurements Predict Residual Survival in Glioblastoma Patients. *Sci Rep*2018;8:14429. [PubMed: 30258190]
131. Swanson KR, Rostomily RC, Alvord EC Jr. A mathematical modelling tool for predicting survival of individual patients following resection of glioblastoma: a proof of principle. *Br J Cancer*2008;98:113–9. [PubMed: 18059395]
132. Rayfield CA, Grady F, De Leon G, et al. Distinct Phenotypic Clusters of Glioblastoma Growth and Response Kinetics Predict Survival. *JCO Clin Cancer Inform*2018;2:1–14.
133. Ellingson BM, Wen PY, Cloughesy TF. Modified Criteria for Radiographic Response Assessment in Glioblastoma Clinical Trials. *Neurotherapeutics*2017;14:307–20. [PubMed: 28108885]
134. Wen PY, Macdonald DR, Reardon DA, et al. Updated response assessment criteria for high-grade gliomas: response assessment in neuro-oncology working group. *J Clin Oncol*2010;28:1963–72. [PubMed: 20231676]
135. Okada H, Weller M, Huang R, et al. Immunotherapy response assessment in neuro-oncology: a report of the RANO working group. *The Lancet Oncology*2015;16:e534–e42. [PubMed: 26545842]
136. Ellingson BM, Sampson J, Achrol AS, et al. Modified RANO, Immunotherapy RANO, and Standard RANO Response to Convection-Enhanced Delivery of IL4R-Targeted Immunotoxin MDNA55 in Recurrent Glioblastoma. *Clinical Cancer Research*2021.

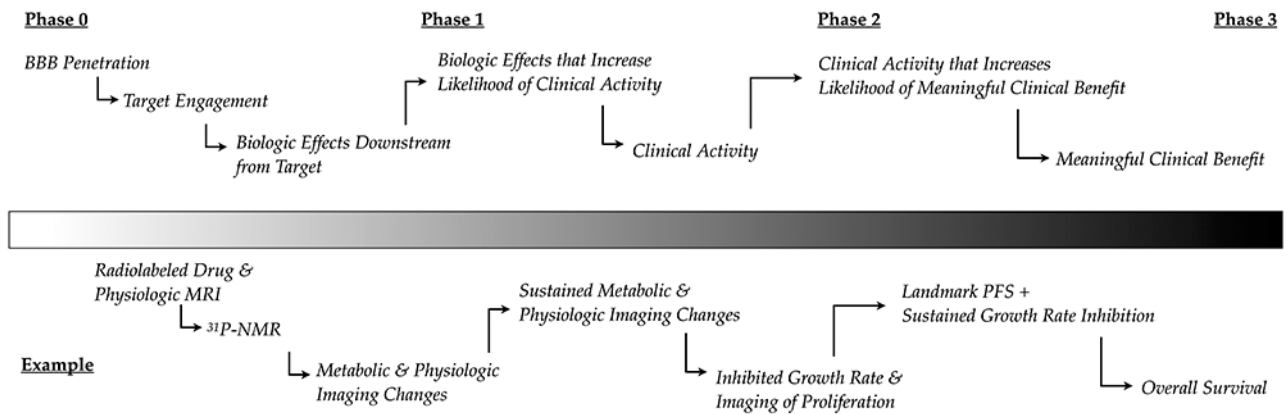


Fig. 1. Relevant Questions and Imaging Strategies for Stages of Drug Development.

Each stage of drug development for high grade gliomas (Phase 0 through Phase 3) has unique questions as well as ways imaging technology can be used to address these questions. During Phase 0 studies questions regarding blood brain barrier (BBB) penetration, target engagement, and downstream biologic effects of the drug are most relevant, which can be quantified through use of radiolabeled drug, metabolic and physiologic imaging technologies. During phase 1 studies, evidence of biologic effects that increase likelihood of clinical activity and evidence of direct clinical activity are pertinent, which can be identified through sustained metabolic or physiologic imaging changes, evidence of inhibited macroscopic (bulk tumor) or microscopic (proliferation) growth rate. In later stage (phase 2-3) trials, clinical activity and increases likelihood of a meaningful clinical benefit and direct evidence of clinical benefit are important, which can be recognized through use of landmark progression-free survival (PFS) benchmarks, sustained growth rate inhibition, and increased overall survival.

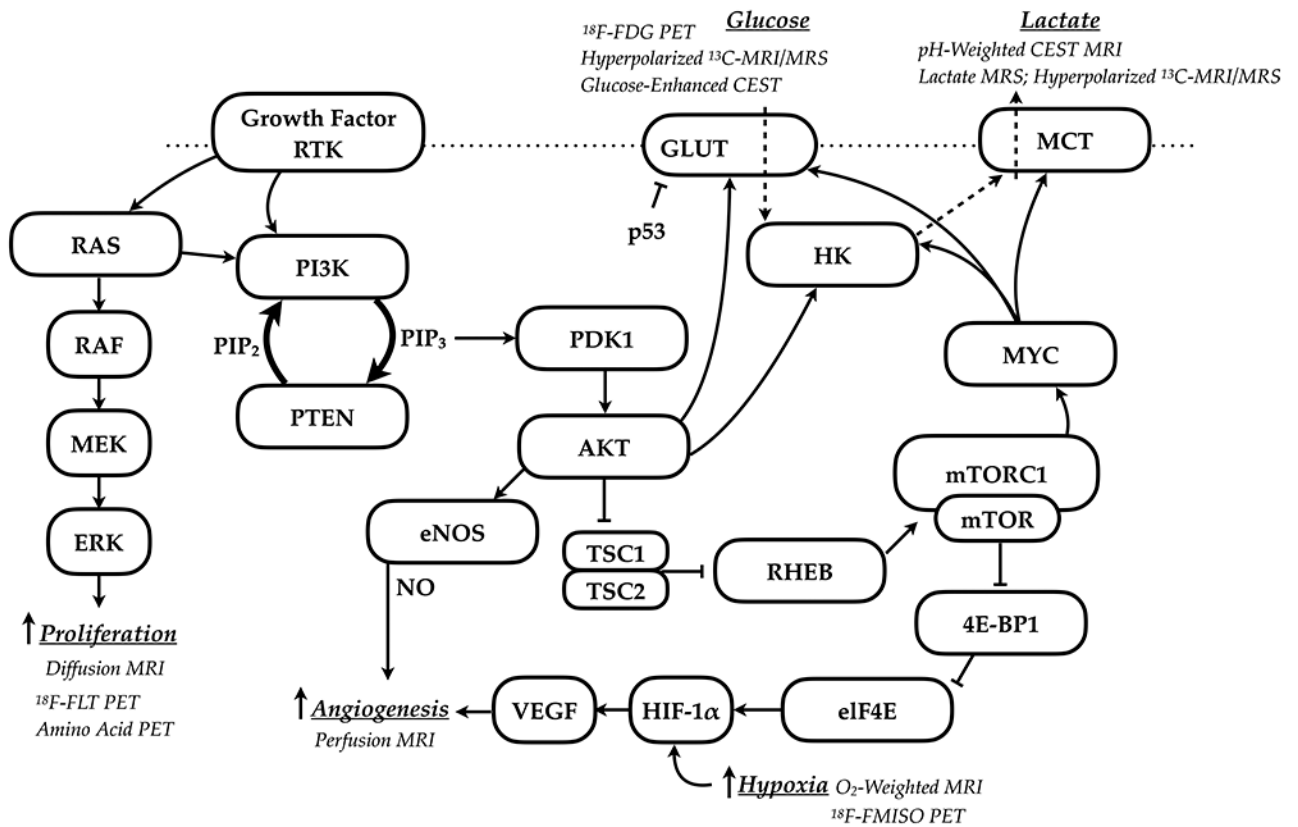


Fig. 2. Example of oncogenic signaling and downstream metabolic and physiologic imaging changes during molecular therapies.

PI3K activation can occur through RAS mutation or increased activation of growth factor receptor tyrosine kinase (RTKs) like EGFR. Activation or mutation of RAS results in stimulation of the RAS/RAF/extracellular signal-regulated kinase (ERK) pathway resulting in increased tumor proliferation. This increase in proliferation can be identified through the use of diffusion MRI, ¹⁸F-fluorothymidine (FLT) PET, or amino acid PET imaging techniques that have been shown to correlate with cellularity and proliferation rates (e.g. ¹⁸F-FET, ¹⁸F-fluorodopa, or ¹¹C-methionine PET). Activation of PI3K/AKT/mTOR pathway after RTK or RAS signaling results in increased angiogenesis through expression of nitric oxide (NO) or through HIF-1 α upregulation and secretion of VEGF. To measure changes in vascularity within the tumor, a variety of perfusion-sensitive MRI techniques can be used including dynamic susceptibility contrast (DSC) or dynamic contrast enhanced (DCE) MRI. Changes in oxygenation within the tumor can also be measured using imaging techniques, including oxygen-sensitive R₂' imaging or radiotracers like ¹⁸F-FMISO that is sensitive to tumor hypoxia. Activation of growth factor RTKs like EGFR also increase glucose metabolism (specific glycolysis) through activation of AKT, MYC, or a variety of other signaling mechanisms. This increase in glucose metabolism can be quantified through the use of ¹⁸F-FDG PET, hyperpolarized ¹³C-glucose or pyruvate, or glucose enhanced CEST imaging (i.e. “glucoCEST”). Lactate and lactic acid production, byproducts of glycolysis, can also be measured using imaging technologies such as pH-sensitive amine CEST MRI, lactate MRS, or hyperpolarized ¹³C-glucose or pyruvate. RTK = receptor tyrosine kinase; MEK = mitogen-activated protein kinase kinase; ERK = extracellular

signal-regulated kinase; PI3K = phosphatidylinositol 3-kinase; PIP₃ = Phosphatidylinositol 3,4,5-triphosphate; PIP₂ = Phosphotidylinositol 4,5-Bisphosphate. PTEN = Phosphatase and tensin homolog; PDK1 = Phosphoinositide-dependent kinase 1; eNOS = enzyme nitric oxide synthase; NO = nitric oxide; TSC1/2 = Tuberous sclerosis complex 1/2; RHEB = Ras homolog enriched in brain; mTOR = Mammalian target of rapamycin; mTORC1 = mTOR complex 1; 4E-BP1 = eukaryotic translation initiation factor 4E-binding protein 1; eIF4E = eukaryotic translation initiation factor 4E; HIF = hypoxia inducible factor; VEGF = vascular endothelial growth factor; LDH = CEST = chemical exchange saturation transfer; FDG = flurodeoxyglucose; FLT = flurothymidine; FMISO = fluoromisonidazole; MRI = magnetic resonance imaging; MRS = magnetic resonance spectroscopy

Author Manuscript

Author Manuscript

Author Manuscript

Author Manuscript

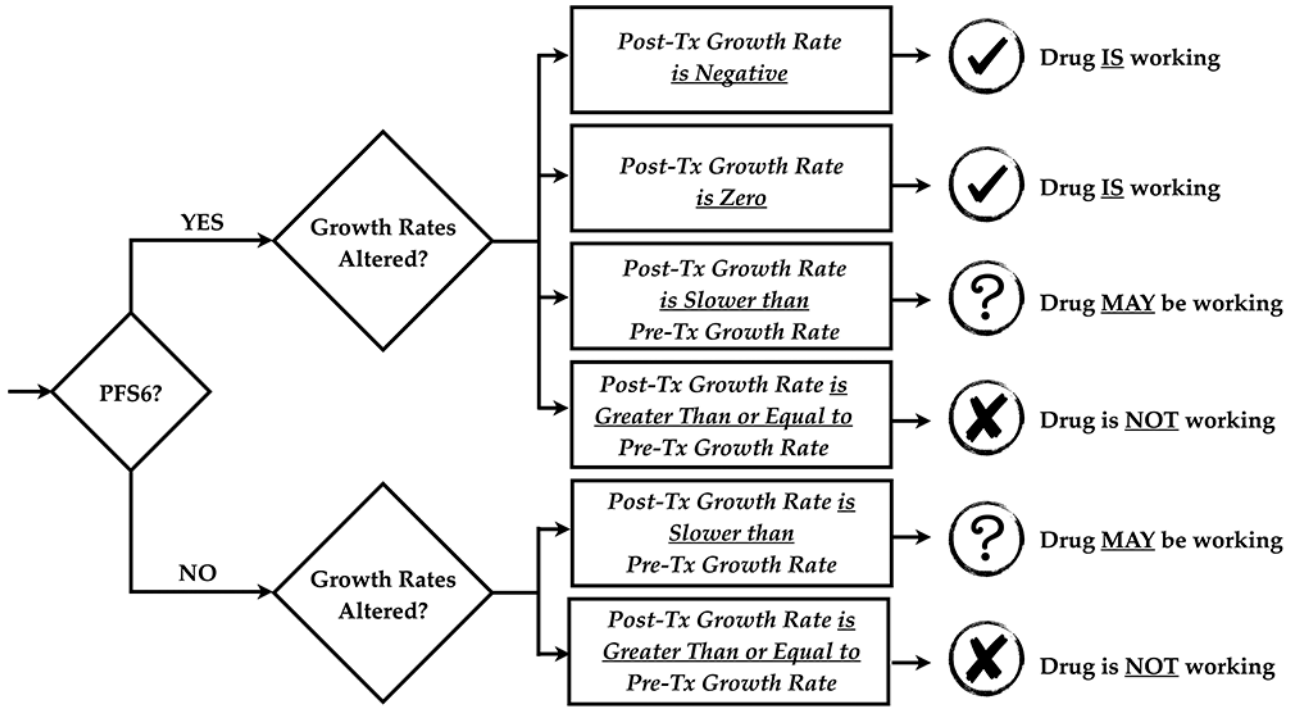


Fig. 3. Framework for determining therapeutic activity in early phase trials. In order to gain confidence that a drug has therapeutic activity that is likely to lead to clinical benefit using a limited dataset in early phase trials, one might consider using landmark progression-free survival (PFS) benchmarks (e.g. PFS6) combined with evidence of altered growth rate trajectory. In patients who reach the PFS benchmark evidence of tumor shrinkage or stabilization would provide confidence the drug is working, whereas if the growth rate has slowed there may be some evidence of activity. Similarly, if patients do not reach landmark PFS but there is evidence the tumor has slowed its growth rate trajectory this may be evidence of therapeutic activity. In these circumstances, adjustments to dose and timing may be appropriate to see clinical benefit.

Author Manuscript

Author Manuscript

Author Manuscript

Author Manuscript

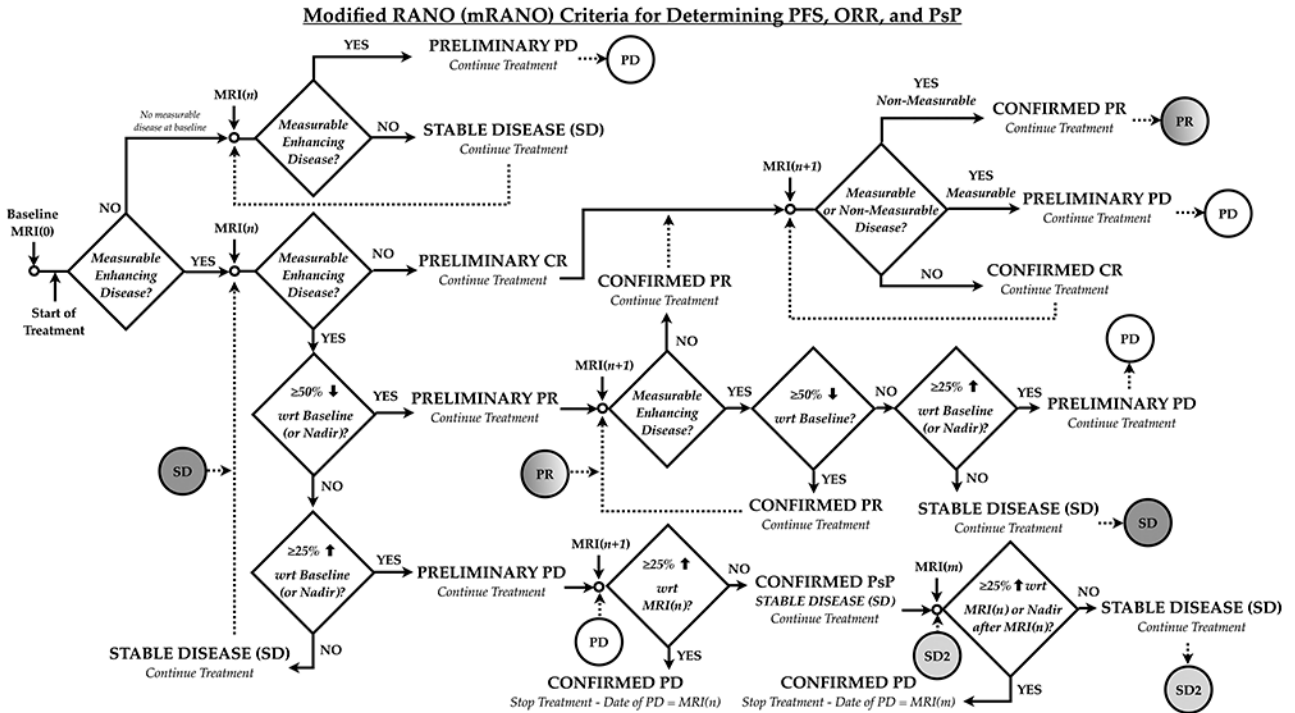


Fig. 4. Modified Response Assessment in Neuro Oncology (mRANO) criteria.
 The mRANO criteria¹³³ was developed as a treatment agnostic criterion for use in patient management and to gain confidence in estimates of PFS and pseudoprogression (PsP) incidence. The primary difference between the mRANO and standard RANO criteria is the requirement to confirm progression on a subsequent examination. ORR = objective response rate; PD = progressive disease; SD = stable disease; PsP = pseudoprogression; PR = partial response; CR = complete response.

Author Manuscript

Author Manuscript

Author Manuscript

Author Manuscript